Geochemical Analysis of the Chinchín Formation in Southern Ecuador

Katherine Ludwig
Augustana College, Rock Island Illinois

Geochemical analysis of the Chinchín Formation in southern Ecuador

a senior thesis written by

Katherine Ludwig

in partial fulfillment of the graduation requirements for the major in geology

Augustana College

Rock Island, Illinois 61201

May 2019

Abstract:

The subduction of the Nazca Plate underneath the South American Plate has led to the uplift of the majority of the Andes Mountains in South America. In Ecuador, the Nazca Plate subducts underneath the North Andes Plate, which collides with the South American Plate. This tectonic setting has formed two parallel mountain chains, the Cordillera Occidental and the Cordillera Real, as well as a complex series of basins between them. However, many of the formations that make up these basins are poorly understood. This study focuses on the Chinchín Formation, an approximately 3.5 km thick, extrusive igneous formation that serves as the bedrock of the Quingeo Basin in southern Ecuador. The Late Cretaceous Yunguilla Formation is believed to unconformably underly the Chinchín Formation and provides a maximum age constraint on the timing of crystallization: 65 Ma (Steinmann et al., 1999). A previous study assigned the Chinchín Formation an Eocene crystallization age, which was determined using zircon fission track (ZFT) dating, but the dating technique was only performed on a single sample from the northern upper third of the Formation, taken from the stratigraphic unit above that studied here. Therefore, the rocks analyzed in this study have an estimated age somewhere between approximately 42.8 and 65 Ma. This study employs XRF analysis to determine the change in composition of an approximately 112 meter range of elevation within the Chinchín Formation in order to better understand the history of basin development in this region. Multiple bedrock samples from the southern portion of the Chinchín Formation were analyzed. Eight bedrock samples as well as one secondary mineral deposit were analyzed. The amygdules present in two non-consecutive samples indicate that this section of the Formation represents portions of at least three different volcanic events, rather than one large or extended event, and that there was secondary mineralogical deposition by low-temperature fluids rich in iron, silica,

and nickel. This secondary mineralogical precipitation occurred after this entire portion of the Formation was deposited, as unusually high iron contents of the rock samples indicate.

Introduction:

The Chinchín Formation is an extrusive volcanic formation in southern Ecuador which serves as the lowest confirmed unit of the Quingeo Basin. Despite having a thickness of ~3.5 kilometers and being located in a very tectonically active region, the Chinchín Formation has only been very minimally studied. Its makeup and variation in rock types were loosely described in the paper which originally separated it from the overlying Tarqui and Quingeo Formations, but no detailed chemical analysis of these formations has yet been performed. The goal of this research is to gain a better understanding of the history and resulting composition of the Chinchín Formation by performing XRF analysis on and studying the textures of a collection of samples from various stratigraphic locations of the exposure. This better understanding will add to the understanding of the history of volcanic activity in the northern Andes Mountains and allow for more in-depth study of the relationships between the Chinchín Formation and other formations in the region, as any compositional changes indicate the conditions under which the rock formed and how it may have been modified in the time since its original crystallization.

Background:

The tectonic activity of the western coast of South America is characterized largely by the subduction of the Nazca Plate beneath the South American Plate, which has led to the formation of the majority of the Andes along South America's western coast. In Ecuador, the Nazca Plate does not directly subduct beneath the South American Plate, but beneath the North

Andes Plate, which then converges with the South American Plate. This paired collision and resulting accreted terranes have led to the formation of two parallel mountain chains, the Cordillera Real, or Eastern Cordillera, and the Cordillera Occidental, or Western Cordillera (Hungerbuhler et al., 2002). The area between these mountain chains, known as the Interandean Valley, contains several basins that have developed in the time since mountain building began in this region.

A 2010 study of uplift in the northern Andes determined that exhumation rates of this segment of the Andes have not been constant over time (Spikings et al.). From 75-55 Ma, there was a rapid exhumation of the Eastern Cordillera, which these authors hypothesize was an immediate reaction to the collision between the Farallon and South American Plate. Other periods of elevated exhumation rates, correlated with tectonic activity, occurred from 45-30 Ma and from 25-18 Ma. During periods of elevated tectonic activity such as these, there is a corresponding increase in volcanic activity, which results in the emplacement of numerous volcanic formations throughout this region. The Chinchín Formation, the focus of this study, is one such formation.

The Chinchín Formation is located in the southern Interandean Valley between the two mountain chains of this portion of the Andes. Figure 1 shows the exact location of the Chinchín Formation exposure within Ecuador, just southeast of the city of Cuenca; and Figure 2 displays a geologic map of the region around Cuenca, Ecuador, including the Chinchín Formation. The Formation is shown in the lower right-hand side of this figure, exposed between the towns of Santa Ana, Quingeo, and Gualaceo.

Fig. 1: Map of Ecuador showing terrain, major cities, and the location of the Chinchín Formation's exposure (red).

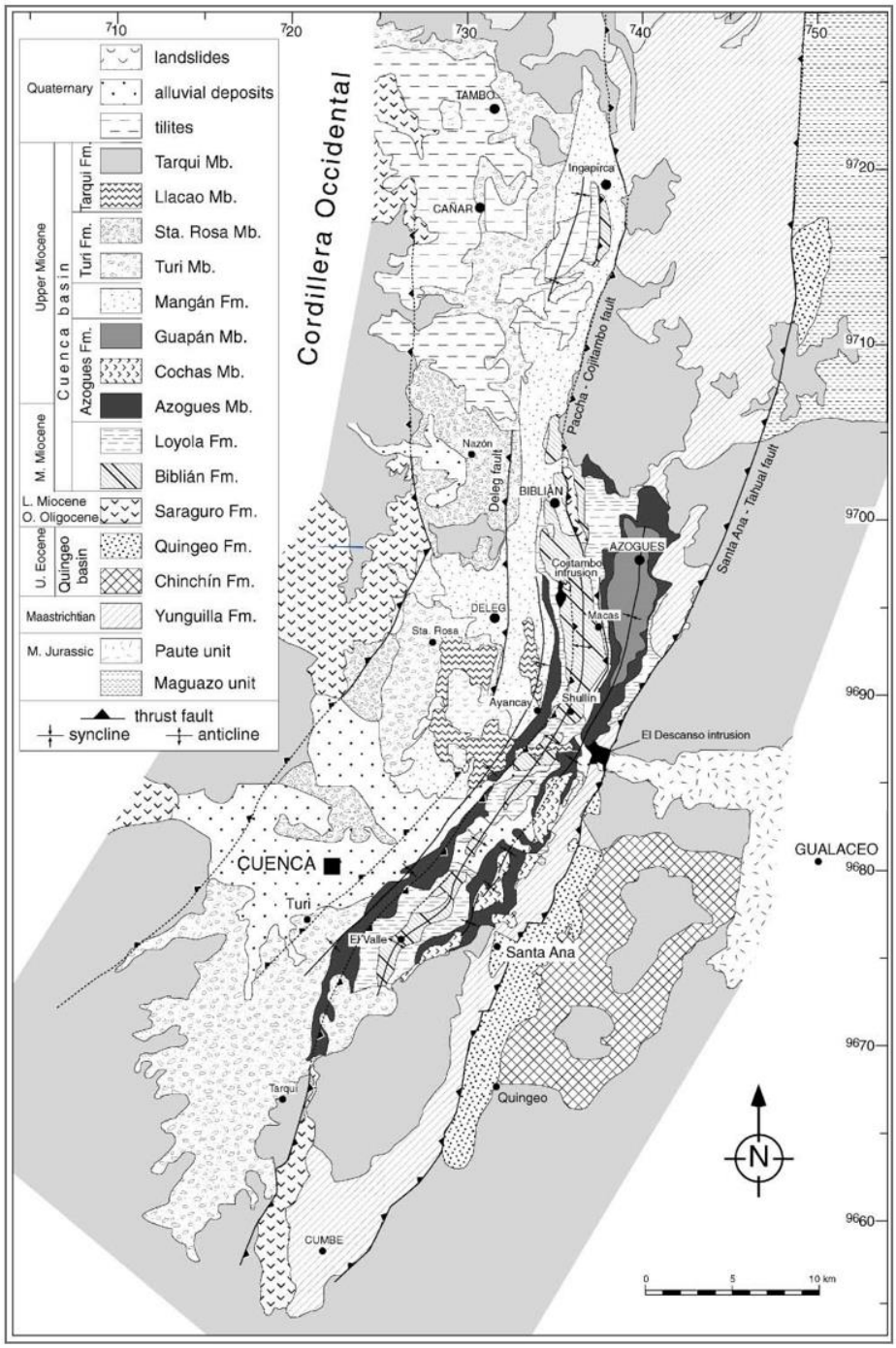

Fig. 2: Geologic map of the Cuenca area (Steinmann 1997).

The Chinchín Formation is an extrusive volcanic formation which forms the basement of the Quingeo Basin. The Chinchín Formation is, at its maximum thickness, between 3500 and 4000m thick and is exposed over a large area to the southeast of Cuenca, Ecuador (Hungerbuhler

et al., 2002). In past studies, this formation was mapped as part of the Tarqui Formation, which is of Miocene age, until the age discrepancy between them was discovered and the Quingeo Formation, an almost entirely sedimentary, fluvial formation, was defined between them (Steinmann 1997). The Tarqui Formation is younger than both the Chinchín and Quingeo Formations by approximately 20 Ma (Hungerbuhler et al., 2002).

While no stratigraphic column yet exists for the Chinchín Formation itself, stratigraphic columns have been created for the Quingeo Basin overall. Two columns are available, one each for the northern and southern regions of the basin. These existing columns focus on the stratigraphy of the sedimentary Quingeo Formation and the volcanic Tarqui Formation, including the existing zircon fission track ages of the stratigraphy. The Chinchín Formation is shown as being a volcanic formation located stratigraphically underneath the Quingeo Formation and as having one ZFT age of 42.8 ± 3.8 Ma, but no further details are provided. These stratigraphic columns are shown in Figure 3.

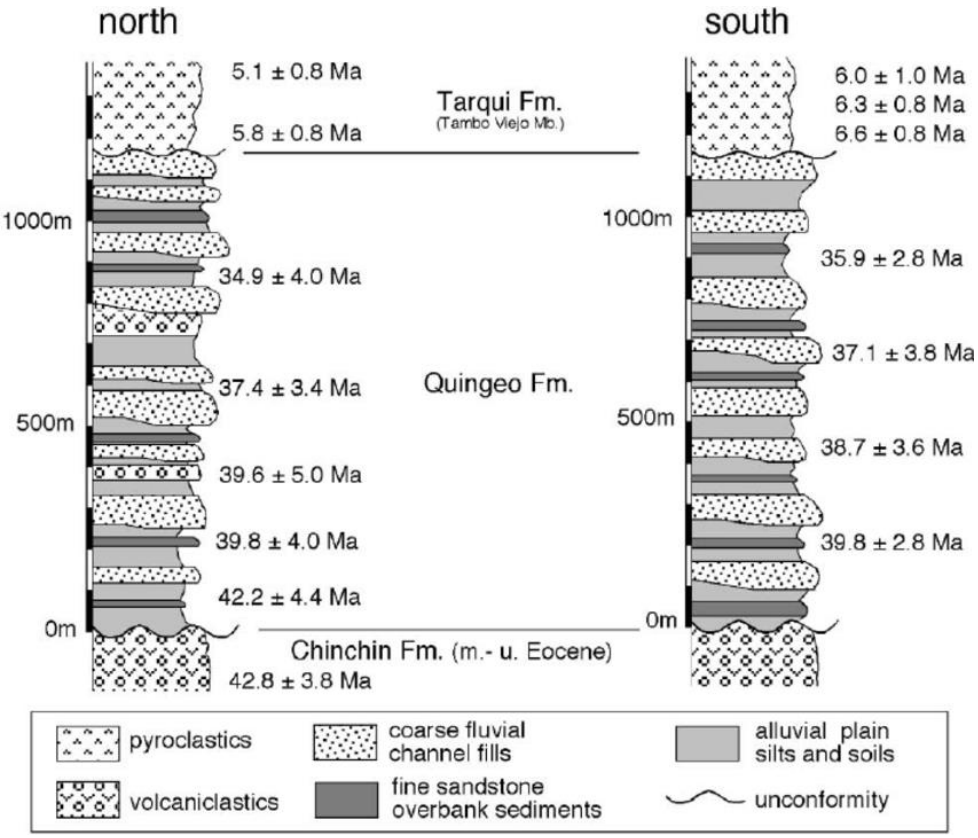

Fig. 3: Stratigraphy of the northern and southern regions of the Quingeo Basin (Hungerbuhler et al., 2002).

The rock types of the Chinchín Formation, while not precisely documented and measured, have also been generally described. The upper third of the Formation is made up of green, andesitic lava flows, which were assigned an Eocene crystallization age using the only rock sample that has been successfully dated in the Chinchín Formation. These andesite flows are underlain by a succession of lava flows and pyroclasts, which show evidence of secondary mineral precipitation. Some beds of conglomerate, up to 5 meters thick, exist between the volcanic rock beds. Finally, the lowest section of the Chinchín Formation is composed of light gray, fine-grained pyroclasts, heavily faulted, with intrusions of finely grained, black basalt with thicknesses of up to 25 meters.

As stated previously, the uppermost portion of the Chinchín Formation is of approximately Eocene age, with a single zircon fission track age determined at 42.8 ± 3.8 Ma. Seven grains were analyzed in total from a sample of andesite taken from the upper third of the formation (Steinmann, 1997; Hungerbuhler et al., 2002). An apatite fission track analysis was also performed on the same sample and yielded an age of 30.5 ± 10.2 Ma. This analysis used 23 apatite grains and is interpreted as relating to the uplift history of the cordilleras and how their depth of burial, and corresponding temperature, has changed (Steinmann, 1997). My samples come from a section of the stratigraphy between this previously analyzed sample and the underlying Yunguilla Formation, which has been dated to 65Ma. While the original intent of this study was to provide more absolute ages of samples from varying elevations within the Formation using zircon U-Pb geochronology, the rock types making up much of the Chinchín Formation are naturally very low in heavy minerals; and it is therefore very difficult to date them using most available methods. While my study will therefore not provide any absolute dates for this portion of the Chinchín Formation, it will be valuable in providing more information on what occurred in the approximate 20 Ma span in which this section of the stratigraphy is believed to have been formed; and it will also encourage more in-depth analysis of the timeline of the evolution of the region in the future.

Methods:

On July 15th, 2018, I collected multiple samples of the volcanic bedrock from the Chinchín Formation's exposure. My goal was to collect approximately 10 bedrock samples from different stratigraphic layers of the Formation by sampling from locations at different elevations. In order to achieve this, I chose a rural road which travels down a mountainside in the southern

portion of the Chinchín Formation's exposure, between the towns of Quingeo and Santa Ana, as my sample area. I was able to take 8 bedrock samples from an elevation change of approximately 112m, ranging from 2728 ± 6m to 2840 ± 6m, as well as an additional mineral sample, Sample 5, which had crystallized in a crack in the rock near sample 4. The location of the sample area for this study is displayed in Figure 4, while Figure 5 displays the sample sites within this sample area.

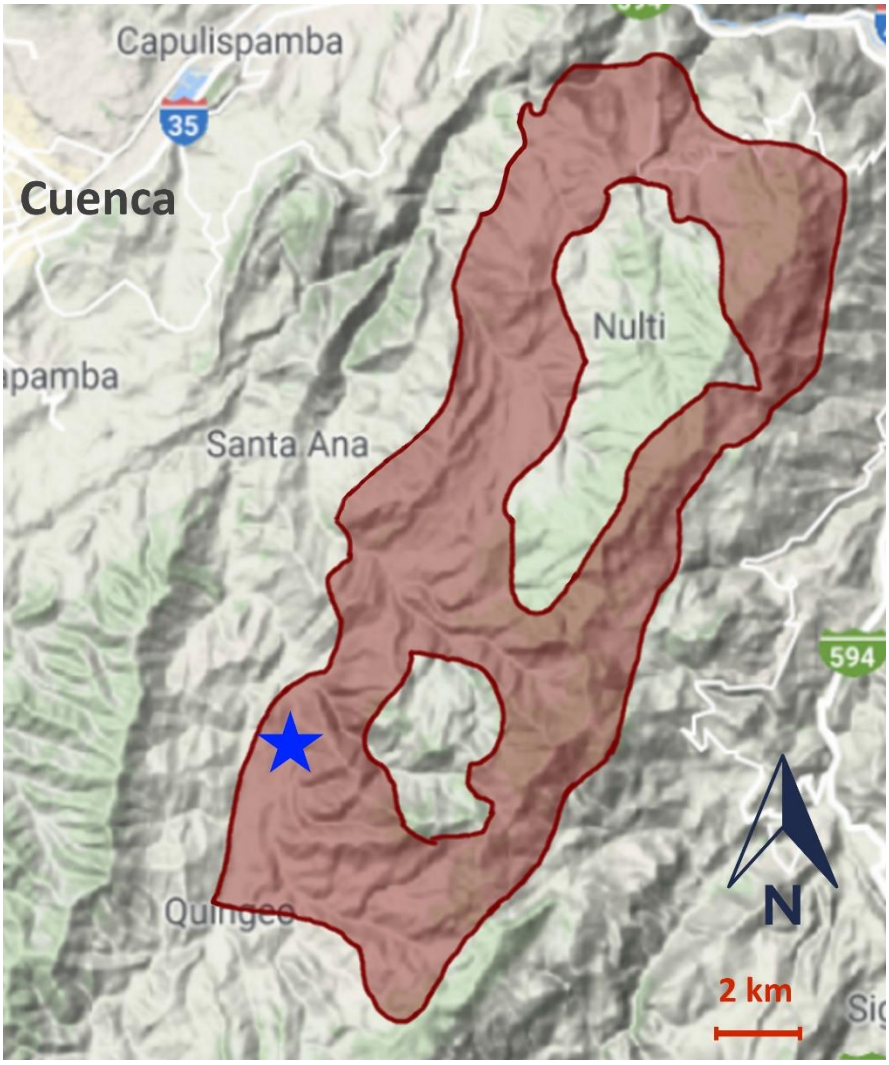

Fig. 4: Location of sample area within the Chinchín Formation. The red area represents that of the Chinchín Formation's exposure, whereas the blue star shows the location of the sample area.

Fig. 5: Locations of bedrock sample sites. Each marker shows the location of a sample site. Sample 1 is located on the far right at the highest elevation, and sample nine is on the far left at the lowest elevation. The elevation range is from 2728 ± 6 to 2840 ± 6 m, a difference of ~112 m.

During sample collection, it is recommended that the outer part of the rock be removed to prevent contamination of other material (Dumitri, 2000); therefore, as I was collecting my samples, I removed approximately the uppermost inch of each sample site's exposure before collecting any rock. I collected enough rock to fill three quarters of a gallon-sized bag for each bedrock sample.

Afterwards, I rinsed off each of my samples with water in order to remove any dust from their surfaces both to reduce the chances of contamination from foreign sediment and in anticipation of possible difficulties in bringing my samples to the United States by plane. Approximately half of my entire volume of samples, including varying portions of all eight rock samples and the entirety of the mineral sample, was permitted back into the United States.

Once my samples were back at Augustana College, they could be processed and melted into fused glass disks to be analyzed using XRF, or X-ray Fluorescence.

XRF analysis works by placing homogenized disks containing the sample, either as pressed pellets or as fused glass disks, in a machine which emits an x-ray beam to excite the electrons present in the elements of the sample and then analyzes the energy produced in order to measure composition. The energy given off is unique to each element, and so the different energy signatures measured by the XRF spectrometer can be used to determine what is present in the sample; similarly, the abundance of the different energy signatures is used to determine how much of each element is present in the sample ("Handheld XRF: How it works").

The first step in this process of preparing my samples for XRF analysis was using a hydraulic jack rock splitter to break the rock samples down to smaller pieces so that they could then be put through a rock crusher, which cannot handle rocks larger than the size of the last digit of the thumb. Each sample was put through the rock crusher approximately ten times in order to maximize pulverization of the rock. The one exception was Sample 3, which was too soft for the crusher and was therefore ground with a mortar and pestle instead.

While mineral separation for U-Pb analysis failed to yield the zircon grains necessary for analysis, the majority of the crushed rock samples remained and was able to be used for chemical analysis. A few grams of the leftover crushed rock of all eight rock samples was milled, as was a similar portion of the mineral sample. This milling was done because pulverization into a homogenous powder both increases the accuracy of compositional analysis and makes easier the process of melting the samples into the fused glass disks for XRF analysis.

The process of milling consisted of filling a small ceramic crucible just high enough with sample to half-cover the zirconium ball within, and then placing that crucible in the shaker mill

for five minutes per sample to thoroughly pulverize it. The crucible and ball were both thoroughly cleaned between samples to avoid contamination between them.

I created 10% fused glass disks for analysis rather than the more concentrated 33% disks because, while the higher sample concentration allows for trace element analysis, the lower concentration of sample lowers the chance of the disk cracking; and these lower-concentration disks can still be analyzed for ten major oxides, including SiO_2, Fe_2O_3, Na_2O, MgO, Al_2O_3, P_2O_5, K_2O, CaO, MnO, and TiO_2, which was sufficient for this study.

To make each of the fused glass disks, 0.64 grams of the sample being analyzed and 6.4 grams of flux were mixed together as homogenously as possible and placed within a small metal crucible. This crucible was placed in a Katanax heater, heated to 1050 degrees Celsius, and poured into a mold. Each disk was allowed to slowly cool down to approximately 80 degrees Celsius before being removed from the mold. The disks were not removed sooner because quicker cooling rates increase the risk of cracking the disk, which would then have to be melted again and recast.

The resulting fused disks were placed in the XRF machine and analyzed three times each along with two standards, DNC-1 and GSP-2. The repeated analyses increase the precision of the results, whereas the standards ensure proper calibration of the machine, as their compositions are known; and in the case of any deviances, the machine could either be recalibrated, or the difference in the data could be corrected mathematically.

In the case of my samples, the data was renormalized to 100%, and some of the values were adjusted mathematically so that the results of the standards were within the range of expected values.

Results:

All of the bedrock samples are porphyritic in texture, which is characteristic of rocks that have been partially cooled below ground before being erupted. Samples 6 and 9 also each contain amygdules, or vesicles which been filled by several different secondary minerals, such as quartz, green chalcedony, and iron deposits. All of these secondary minerals have concentric growth patterns.

Using the XRF data, the samples were sorted into rock types based on silica content and combined sodium oxide and potassium oxide contents. The resulting rock types were two basaltic andesites, samples 1 and 2; five andesites, samples 3, 4, 7, 8, and 9; and one dacite,sample 6. These rock types can be seen plotted in Figure 6.

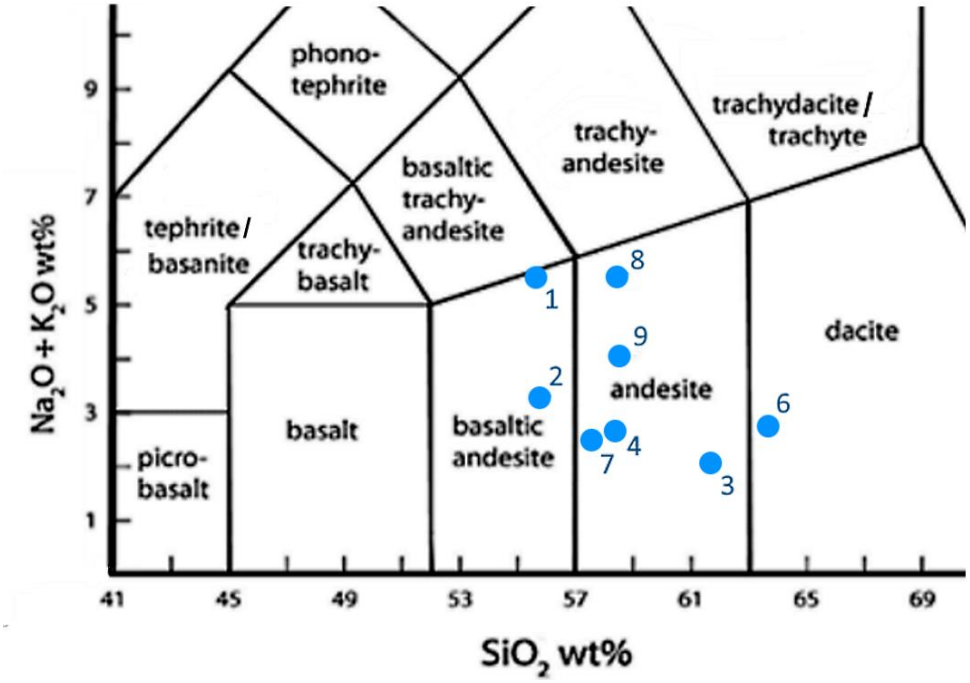

Fig. 6: Identifications of rock samples based on SiO_2, Na_2O and K_2O concentrations.

After sorting the rock samples into different rock types, I graphed the concentrations of several of the oxides in order to look for any changes and trends in these changes that might exist in relation to elevation change. Despite significant variation, there was no clear relation between

elevation and oxide concentration of SiO_2, although it was significantly higher in samples 3 and 6, two of the samples most visibly affected by the secondary mineral precipitation and reworking of the material (Figure 7). The concentrations of sodium and potassium oxides, combined in Figure 8, show a relationship more or less inverse to that of the silica content in the rocks. The iron (III) oxide content, Fe_2O_3, which is consistently elevated in all samples, shows a positive trend with elevation increase in this portion of the Chinchín Formation's exposure (Figure 9). Manganese oxide, MnO, is present in consistently low concentrations, but is present in significantly higher weight percentages in samples 6 and 9, which are the two samples containing visible amygdules. In these composition change graphs, Sample 1 is furthest to the right, being highest in elevation; and Sample 5 was disincluded, as it is a mineral sample rather than a bedrock sample.

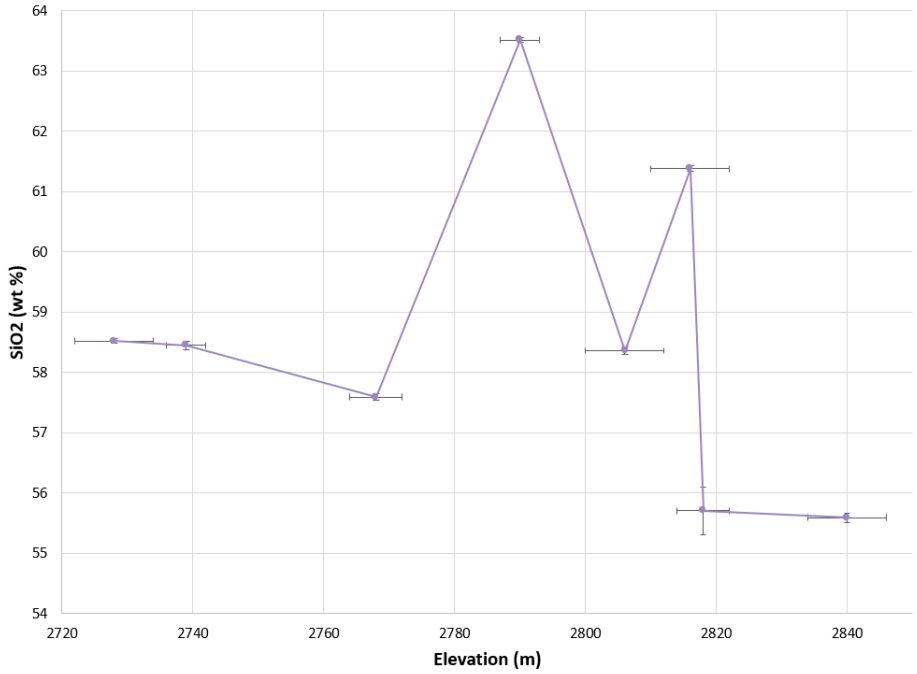

Fig. 7: SiO_2 concentration changes with elevation in bedrock samples from an ~112m section of the Chinchín Formation. Sample 1 is highest in elevation.

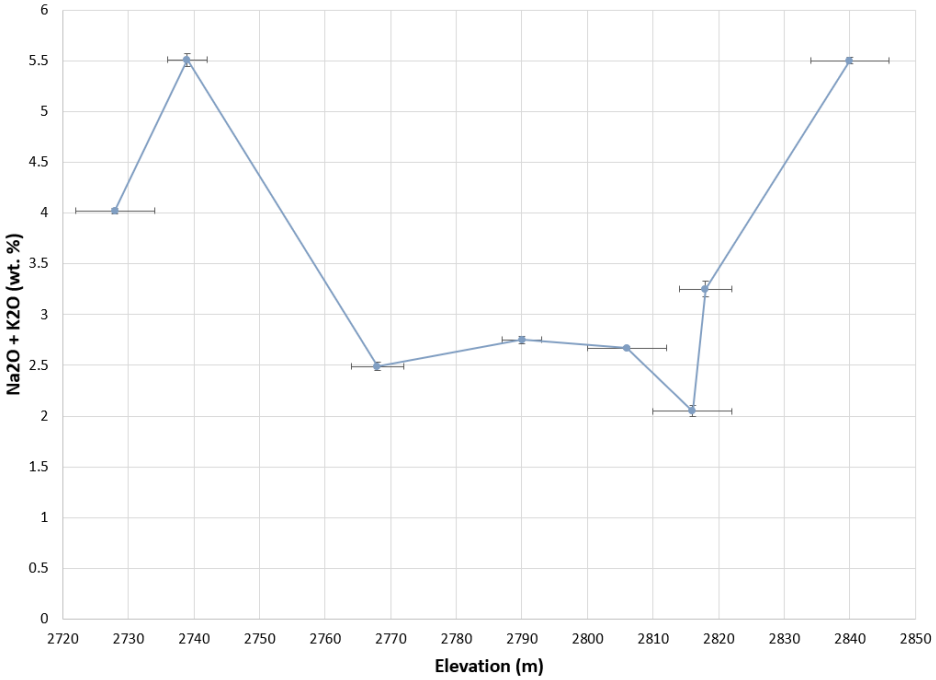

Fig. 8: Na_2O and K_2O combined concentration changes with elevation in bedrock samples from an ~112m section of the Chinchín Formation. Sample 1 is highest in elevation.

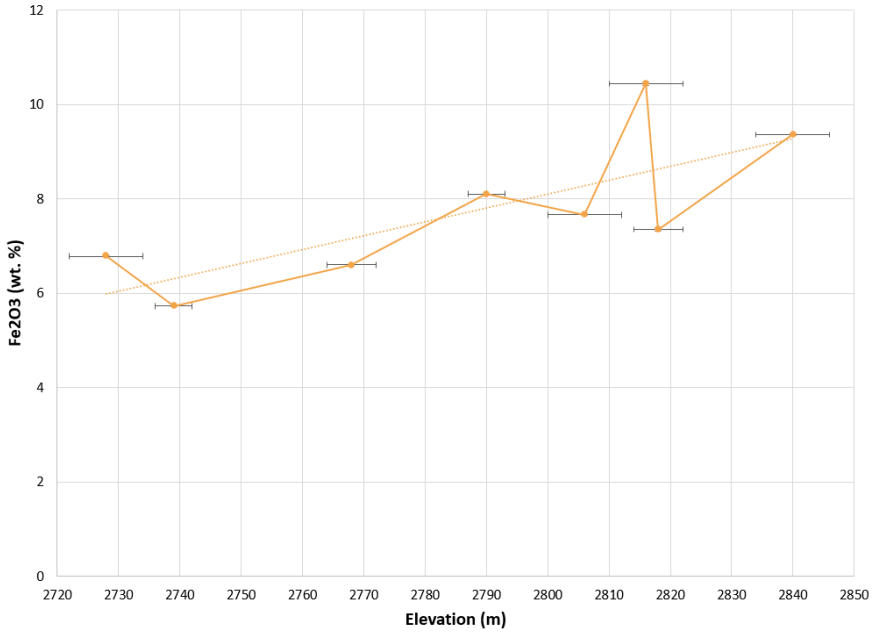

Fig. 9: Fe_2O_3 concentration changes with elevation in bedrock samples from an ~112m section of the Chinchín Formation. Sample 1 is highest in elevation. A trendline shows the positive correlation between Iron (III) content and elevation.

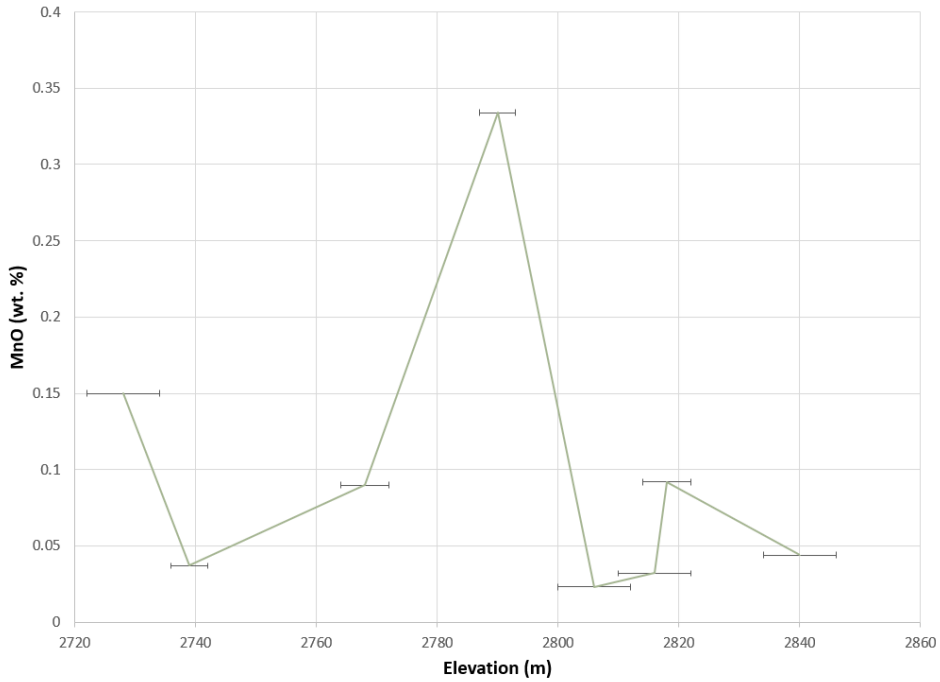

Fig. 10: MnO concentration changes with elevation in bedrock samples from an ~112m section of the Chinchín Formation.

Conclusions:

The compositions and textures of the rock samples collected from the Chinchín Formation for this study support the interpretation that these rocks were formed in a continental setting during volcanism resulting from the subduction of the Farallon Plate. Although the samples range in composition from basaltic andesite to dacite, most of the samples are andesites. Continental volcanic arc environments commonly form rocks of intermediate composition, and the volcanic material tends to be hydrous and to erupt in explosive volcanic events. The presence of bubbles in two of the samples in this study shows that these rocks were in fact hydrous, and the commonality of pyroclastics and tuffs in the stratigraphy indicates an explosive volcanic environment.

Among the eight bedrock samples in this study, there are parts of most likely no less than three separate lava flows preserved. Sample 6, an amygdaloidal dacite, and Sample 9, an amygdaloidal andesite, likely document the tops of two different volcanic flows. The vesicles which later filled in with secondary minerals are usually found at the top of volcanic flows, as the gas bubbles are low in density and float near the top of the lava. Of course, as this part of the Andes Mountains has been subject to significant deformation due to its tectonic environment since the time of emplacement, it is possible that these layers have been significantly folded or overturned, and that Sample 9 therefore documents the end of the volcanic event which deposited some of the rock which is now higher in elevation than it , but this is a much less likely possibility.

In order to analyze the concentrations of individual oxides in the bedrock samples analyzed for this study, the XRF analysis results of these samples were compared to the average concentrations of these oxides within the rock type that each sample was designated (Carpenter and Keane, 2016). Many of the oxides were close to the average for these rock types, but there were some exceptions. The most dissimilar to the expected values was iron (III) oxide, Fe_2O_3, whose concentration in the samples was in some instances nearly three times that of the average concentration for the corresponding rock type. These differences are most likely due to iron additions during low-temperature fluid reworking of the material, but they may also reflect some overall changes in the magma composition. There was a tendency towards higher iron contents as elevation increased, which could be either due to crystal fractionation and an overall change in magma composition; or it could be a result of the larger amounts of the iron deposited as ion-rich fluid reworked the material staying in the upper layers of the stratigraphy rather than reaching deeper rock.

There was also a significant positive relationship between SiO_2 and MnO contents and the presence of amygdules in the rock. The concentrations of both of these oxides were likely increased in all of the rock samples, like that of iron (III) oxide. Due especially to the addition of SiO_2 to the rocks, some of the samples analyzed here likely would have originally plotted at slightly different compositions and even rock types. Sample 6, for example, was one of the most significantly compositionally altered samples due to its small, deformed and impossible to remove amygdules as well as high amounts of weathering. This sample currently plots as a dacite, but it was most likely originally an andesite or even a basaltic andesite.

Sample 3 is another significantly chemically altered bedrock sample. The weight percentages of iron (Fe_2O_3), feldspar, and silica within Sample 3 are consistently, significantly different from the two samples nearest to it in elevation, Samples 2 and 4. This is likely due to the heavier amounts of weathering on this sample, which has removed portions of certain components more than others and therefore altered its overall composition. This weathering may have also made it easier for fluid flow to deposit secondary minerals within this sample's structure, further altering its overall composition.

Sample 5, the mineral sample which I collected near bedrock Sample 4, is largely hematite, but also contains other minerals that precipitated from the same low temperature fluid that deposited the minerals in the amygdules of samples 6 and 9 and altered the composition to varying extents of all of the bedrock samples. The fact that this sample existed precipitated in a crack in the rock shows that some significant deformation of this section of the stratigraphy had already taken place by the time these minerals were precipitated, or by the time they had finished precipitating.

It would be a reasonable conclusion to surmise that the section of the Chinchín Formation stratigraphy studied in this project was deposited in a relatively short period of time, as only an ~112 meter portion of the ~3.5 kilometer thick formation was analyzed, and the entire Formation is estimated to have formed during a 20-million-year time span. This time span was during a period of increased uplift in this region of the Andes, which could have in turn caused a significant increase in magmatism as the subduction of the Farallon Plate caused the partial melting of the mantle that led to the Chinchín Formation's emplacement.

Based on the stratigraphy of the Chinchín Formation, a general history of the deposition and alteration of the lithology can be extrapolated. The first rocks to be deposited were light gray, fine-grained pyroclasts that were brought to the surface in an explosive volcanic eruption, or in a consecutive series of these eruptions, in a continental volcanic arc environment. This rock solidified and was later faulted due to the continued compressive forces of the tectonic activity in the region. These faults were filled and made larger by intrusions of black basalt, some of these dikes being up to 25 meters thick. Afterwards, more volcanic material was erupted, including tuffs, more pyroclasts, and lava flows of majority intermediate composition. Between some of the volcanic events documented here, fast flowing rivers formed and deposited conglomerates with large, cobble-sized clasts. Later, this section of the stratigraphy was affected by low-temperature secondary mineral precipitation due to the flow of fluids containing high amounts of dissolved ions, resulting in the formation of amygdules and overall composition shifts of the rock itself. Most likely, the silica-rich minerals, chalcedony and quartz, formed before the more fragile and easily lost concentrically formed iron deposits. Some of the fluid flow was likely also rich in manganese, which would account for the significantly higher concentration of that element in the samples containing amygdules in comparison with the less porous and less altered

samples. Finally, around 42 million years ago, according to the existing ZFT date for this formation, a large volume of andesitic lava flows was deposited, accounting for approximately a third of the Chinchín Formation's total thickness. The entirety of the Chinchín Formation was then slowly uplifted as the subduction of the Farallon and later Nazca Plates continued, large portions of the stratigraphy being eroded away as younger sedimentary facies and volcanic flows were deposited on top until it reached the elevation and developed the exposure it has today.

Potential future work for the samples used in this study and the Chinchín Formation in general include constructing a stratigraphic column for the Formation, SEM analysis, and dating more samples from the Formation. Studying the exact measurements and rock types within the Chinchín Formation and constructing a stratigraphic column for the Formation would allow future experiments to be better related to one another, as the relative locations of different samples would be easier to compare in a geologic rather than geographic context; and the column would provide a reference to make easier the process of choosing portions of the stratigraphy to collect samples from for different types of analyses. SEM work, meanwhile, could be used to analyze different parts of the rocks and determine which minerals are present, not only the oxides. This information can be used to figure out more exactly the composition of these rocks and of the minerals later precipitated in them, potentially giving a better idea of how their compositions have been altered and what they may have originally been. Collecting more samples from this formation to date would also be beneficial in gaining a better understanding of how this formation relates to those around it. While the samples that I collected were unable to be dated by my chosen means, a sample from the section of the stratigraphy above them has been successfully dated. Therefore, further samples from the same section of the stratigraphy, which

accounts for approximately a third of the total thickness, could establish the range of dates over which this section of the stratigraphy was formed.

References Cited:

Anonymous. Handheld XRF: How it Works: https://www.bruker.com/products/x-ray-diffraction-and-elemental-analysis/handheld-xrf/how-xrf-works.html (accessed April 10, 2019).

Carpenter, M.B., and Keane, C.M., 2016, The Geoscience Handbook 2016: American Geosciences Institute, p. 209-210.

Dumitri, T.A., 2000, *Quaternary Geochronology: Methods and Applications*: American Geophysical Union, p. 131-162, doi: 10.1029/RF004p0131.

Hungerbühler, D., Steinmann, M., Winkler, W., Seward, D., Egüez, A., Peterson, D.E., Helg, U., and Hammer, C., 2002, Neogene stratigraphy and Andean geodynamics of southern Ecuador: Earth Science Reviews, v. 57, p. 75-124, doi: 10.1016/S0012-8252(01)00071-X.

Steinmann, M., 1997. The Cuenca basin of southern Ecuador: tectono-sedimentary history and the Tertiary Andean evolution. PhD Thesis, Institute of Geology ETH Zurich, Switzerland, 176 pp.

Steinmann, M., Hungerbühler, D., Seward, D., and Winkler, W., 1999, Neogene tectonic evolution and exhumation of the southern Ecuadorian Andes: a combined stratigraphy and fission-track approach: Tectonophysics, v. 307, p. 255-276, doi: 10.1016/S0040-1951(99)00100-6.

Spikings, R.A., Crowhurst, P.V., Winkler, W., and Villagomez, D., 2010, Syn- and post-accretionary cooling history of the Ecuadorian Andes constrained by their in-situ and detrital

thermochronometric record: Journal of South American Earth Sciences, v. 30, p. 121-133, doi: 10.1016/j.jsames.2010.04.002.